Determination of volumetric gas–liquid mass transfer coefficient of carbon monoxide in a batch cultivation system using kinetic simulations

Nulee Jang, Muhammad Yasin, Shinyoung Park, Robert W. Lovitt, In Seop Chang

PII: S0960-8524(17)30662-4
DOI: http://dx.doi.org/10.1016/j.biortech.2017.05.023
Reference: BITE 18049

To appear in: *Bioresource Technology*

Received Date: 21 February 2017
Revised Date: 30 April 2017
Accepted Date: 3 May 2017

Please cite this article as: Jang, N., Yasin, M., Park, S., Lovitt, R.W., Chang, I.S., Determination of volumetric gas–liquid mass transfer coefficient of carbon monoxide in a batch cultivation system using kinetic simulations, *Bioresource Technology* (2017), doi: http://dx.doi.org/10.1016/j.biortech.2017.05.023

Determination of volumetric gas–liquid mass transfer coefficient of carbon monoxide in a batch cultivation system using kinetic simulations

Nulee Jang[1¶], Muhammad Yasin[2¶], Shinyoung Park[1], Robert W. Lovitt[3] and In Seop Chang[1*]

[1] School of Earth Sciences and Environmental Engineering, Gwangju Institute of Science and Technology (GIST), Gwangju 61005, Korea
[2] Department of Chemical Engineering, COMSATS Institute of Information Technology (CIIT), Lahore, Pakistan
[3] College of Engineering, Center of Complex Fluids Processing, Multidisciplinary Nanotechnology Centre, Swansea University, Swansea, SA2 8PP, UK
¶ Equally contributed
[*] Corresponding author. Tel.: +82 62 715 3278; Fax: +82 62 715 2434. E-mail address: ischang@gist.ac.kr (I.S. Chang).

Abstract

A mathematical model of microbial kinetics was introduced to predict the overall volumetric gas–liquid mass transfer coefficient (k_La) of carbon monoxide (CO) in a batch cultivation system. The cell concentration (X), acetate concentration (C_{ace}), headspace gas (N_{co} and N_{co_2}), dissolved CO concentration in the fermentation medium (C_{co}), and mass transfer rate (R) were simulated using a variety of k_La values. The simulated results showed excellent agreement with the experimental data for a k_La of 13 /hr. The C_{co} values decreased with increase in cultivation times, whereas the maximum mass transfer rate was achieved at the mid-log phase due to vigorous microbial CO consumption rate higher than R. The model suggested in this study may be applied to a variety of microbial systems involving gaseous substrates.

Keywords: Carbon monoxide, Gas–liquid mass transfer, Kinetic simulation, *Eubacterium limosum* KIST612, Batch cultivation

1. Introduction

Fossil fuel refinery has been a major source for global energy production. The predicted scarcity, uneven regional distribution, and greenhouse gas emissions have triggered the use of clean technologies for fossil fuels, and to explore alternate energy resources (Verma et al., 2016). Microbial synthesis gas (syngas) fermentation is a very promising technology in this context; since, it employs biological catalysts to convert syngas into platform chemicals, and clean energy biofuels (Munasinghe & Khanal, 2010). Syngas; a mixture of carbon monoxide (CO), hydrogen (H_2), carbon dioxide (CO_2), can be produced by the gasification of fossil (e.g., coal) and renewable energy resources (e.g., biomass). The versatility of feedstock for syngas production, and its availability in waste streams from thermal power plants, iron works and various chemical processes (Yasin et al., 2015) make it superior choice over agroenergy crops for biorefinery (Ramachandriya et al., 2016).

Bioprocess scale-up for microbial syngas utilization relies on efficient gas-liquid mass transfer of syngas (CO, in particular) in fermentation medium (Bredwell et al., 1999; Garcia-Ochoa & Gomez, 2009; Yasin et al., 2015). Syngas-utilizing bacteria uptake the gaseous substrates in the dissolved state. The dissolved gas concentrations in the fermentation medium depend on the ability of the bioreactor to deliver gas to the reaction system (Doran, 1995; Garcia-Ochoa & Gomez, 2009). The mass transfer rate of bioreactor system dependent on two important parameters: driving force (C^*- C_{CO}) and volumetric gas-liquid mass transfer coefficient (k_La). The determination of aforementioned parameters is a prerequisite to devise scale-up strategies for syngas fermentation (Jeong et al., 2016). This requires online monitoring and measurement of dissolved CO (C_{CO}) levels, which is not possible for relatively small systems such as vial and tube culture owing to limited sample volume, configurational limitations and unavailability of online monitoring equipment.

Kinetic modeling has been a valuable tool to predict the nature and control of gas

fermentation processes. A variety of kinetic and statistical models have been suggested for predicting microbial growth, substrate consumption, metabolite formation, and other parameters associated with the biological processes central to a variety industrial applications (Mohammadi et al., 2014). Among the growth kinetic models, Monod model is widely employed to a variety of microbial reaction systems; since, it reflects the most characteristic features of microbial growth quite well particularly in exponential and stationary phases (Allman, 2011). However, Monod model underestimates the growth rates at low substrate concentrations, while maximum specific growth rates (μ_{max}) are achieved too slowly at the high substrate concentrations (Kovárová-Kovar & Egli, 1998). For these reasons, it is desired to incorporate the most influential parameters in Monod model for true representation of batch fermentation. Previously, the Monod equation has been modified to incorporate parameters such as substrate and/or product inhibition (Han & Levenspiel, 1988). It can also be applied from simple batch cultures to continuous systems similar to those examined in the current study (Vega et al., 1989a; Vega et al., 1989b).The versatility of this model renders it adaptable to a variety of biological systems and processes.

Conventional models for predicting dynamic behaviors of microbial systems rely on the fully dissolved substrates (such as sugars and organic acids). These concentrations may be readily quantified using instrumental analyzing techniques; however, simulating microbial systems of gas-utilizing microorganisms, such as carboxydotrophs and methanotrophs remains still challenging due to difficulty in measuring the C_L values (Jeong et al., 2016; Yasin et al., 2015). Researchers have estimated C_L values, using Henry's law to simulate CO fermentation processes (Mohammadi et al., 2014; Younesi et al., 2005). However, the actual dissolved gas concentrations do not fit well to the theoretically predicted values by Henry's law at all partial pressures due to the continuous consumption of dissolved gas by the microorganisms (Jeong et al., 2016). Therefore, predictions of kinetic parameters using

saturated concentration (C^*) from Henry's law may result in inaccurate microbial activity estimates. Notably, the dissolved gas concentrations are highly dependent on k_La and the gas partial pressure (Doran, 1995; Garcia-Ochoa & Gomez, 2009; Yasin et al., 2014). The potential factors that influence the mass transfer can be incorporated to develop analytical or mathematical models that can be used for time-course estimation of C_{CO} levels, and required k_La to achieve those C_{CO} levels during fermentation.

In previous studies, dimensional analysis was used to normalize the mass transfer data, and to predict the k_La values (Ahmed & Semmens, 1992; Munasinghe & Khanal, 2012). No study has yet been reported to predict the actual k_La that produces real time dissolved gas concentration (C_L) levels in the system. The actual C_{CO} values are important for determining precise microbial activity, in terms of microbial growth and product formation (Merchuk & Asenjo, 1995). Thus, the microbial kinetic parameters are incorporated into the gas–liquid mass transfer kinetics (Merkel & Krauth, 1999; Vega et al., 1989a; Vega et al., 1989b).

In this study, gas-liquid mass transfer parameters and modified Monod model were employed to simulate the kinetics of batch microbial cultivation system fed with CO. Time course microbial growth, product formations, and CO consumptions were simulated by predicting the required k_La. Finally, saturated and dissolved CO concentrations; mass transfer rate, and specific CO consumption rates were simulated to represent their variations during batch fermentation.

2. Materials and methods

2.1. Strain and culture

Eubacterium limosum KIST612 was used as a model strain to simulate batch cultivation using CO substrate (Chang et al., 1997). The composition of the fermentation medium, the growth characteristics of the bacterium, and conditions for strain cultivation can be found elsewhere (Chang et al., 1999).

2.2. Quantification of cell growth and products

The cell concentrations, and products (CO_2, and acetic acid) data used in this study are adopted from previous study (Chang et al., 1999). Standard methods were used for the quantification of cell concentration, acetic acid and CO and CO_2.

2.3. Product inhibition constant

The product inhibition constant of the undissociated acetic acid was determined using the cultivation under different concentrations of sodium acetate (0–480 mM) and a fixed pressure of 1 atm CO. The specific growth rate (μ) for each acetate concentration was measured to determine the effect of product inhibition on microbial growth.

2.4. Kinetic model

The mathematical model equations were developed to describe the batch system with gas substrate. All numerical simulations and statistical analyses were performed using Microsoft Excel 2016.

The Monod kinetic model may be used to describe microbial growth under significantly substrate-limited conditions, such as in vial cultures that cannot maintain a high mechanical agitation speed. In this study, the substrate inhibitory effect of CO was not considered. Therefore, the model began as follows:

$$\mu = \frac{\mu_{max} \cdot C_{co}}{K_S + C_{co}} \quad (1)$$

Where K_S is the substrate saturation constant (mM)

Several organic acid products, such as acetic acid or butyric acid, were produced in the liquid medium, and were present in undissociated forms that could easily pass through the cellular membrane. The undissociated acids that diffused into the cells changes the intracellular pH. Cell death during cultivations is accelerated by high product inhibition. Because Eqn. 1 did not contain terms relating to the effects of cell death and product inhibition, it was modified by introducing the product inhibition constant of acetate (K_P) and

the endogenous cell death coefficient (K_d), as follows:

$$\mu = \frac{\mu_{max} \cdot C_{co,}}{(K_S + C_{co})} - K_d \cdot \left(1 + \frac{C_{ace}}{K_P}\right) \quad (2)$$

Product inhibition influences not only the cell death rate, but the growth rate of living cells; therefore, the cell growth term was modified to include a non-competitive product inhibition form as follows:

$$\mu = \frac{\mu_{max} \cdot C_{co}}{(K_S + C_{co}) \cdot (1 + C_{ace}/K_P)} - K_d \cdot \left(1 + \frac{C_{ace}}{K_P}\right) \quad (3)$$

The formation of the cell mass (dX/dt) was expressed as a function of the cell concentration as follows:

$$\frac{dX}{dt} = \mu \cdot X \quad (4)$$

Under the experimental conditions, there is no need to use complex equation of state (EOS) because the behavior of real gas molecules may be modeled as an ideal gas. The CO partial pressure (P_{co}) was predicted from the simulated CO (N_{CO}) present in the headspace using the ideal gas law to simplify the conversion:

$$P_{co} = N_{CO} \cdot 0.082 \cdot (273.15 + T)/V_g \quad (5)$$

Where T is the temperature (K), V_g is the headspace volume (L)

The gas–liquid mass transfer parameter was introduced to predict the dynamic behavior of CO as a substrate. A saturated concentration of the dissolved CO ($P_{co} \cdot H_{co}$) was estimated using Henry' law. Finally, the change in dissolved CO concentration by time became:

$$\frac{dC_{co}}{dt} = k_L a \cdot (P_{co} \cdot H_{co} - C_{co}) - \mu \cdot X/Y_{X/co} \quad (6)$$

Where H_{co} is Henry's constant of CO (mmol/L/atm), $Y_{X/co}$ is yield coefficient of cell mass from CO (mg/mmol), P_{co} is CO partial pressure in headspace (atm)

N_{CO} was simulated based on the dissolved CO consumed in the broth(V_L) as follows:

$$\frac{dN_{co}}{dt} = -V_L \cdot \mu \cdot X/Y_{X/co} \quad (7)$$

CO_2 in the headspace (N_{co_2}) was simulated by combining the CO consumed in the medium with the CO_2 yield on CO ($Y_{CO_2/CO}$):

$$\frac{dN_{co_2}}{dt} = Y_{CO_2/co} \cdot V_L \cdot \mu \cdot X/Y \quad (8)$$

In the same way, acetate production was simply predicted from the microbial CO consumption through the acetate yield coefficient on CO ($Y_{ace/CO}$):

$$\frac{dC_{ace}}{dt} = Y_{ace/co} \cdot \mu \cdot X/Y_{X/co} \quad (9)$$

The initial conditions used for each model are provided in Table 1.

3. Results and discussion

3.1. The effect of acetate on the specific growth rate of *E. limosum* KIST612

The accumulation of end products, such as organic acids and alcohols, can considerably affect the specific growth rate of cells in a fermentation system (Lin et al., 2008; Wang & Wang, 1984; Zhang et al., 2016). The growth inhibitory effect usually increases linearly in proportion to the organic acid concentration. The cell growth of *E. limosum* KIST612 is also inhibited by high acetate concentrations (Chang et al., 1998). In this study, acetate does not appear to inhibit cell growth at low concentrations up to 120 mM. Beyond this limit, cells grow more slowly. Inhibition of the specific growth rate was nearly linear up to 480 mM. These data were used to extrapolate the cell growth inhibition beyond 120 mM to obtain a maximum specific growth rate at 240, 360, and 480 mM to predict the product inhibition constant (K_P). The extrapolation suggested that *E. limosum* KIST612 could not grow at/above 744 mM sodium acetate in the medium. At this concentration, 4.2 mM of the total acetic acid was present in an undissociated form. This concentration was considered to provide an acetate inhibition constant of *E. limosum* KIST612 in the neutral pH range. Although the batch culture investigated in this study did not achieve a high titer of acetic acid, this constant was necessary for predicting the microbial kinetics and behaviors of gas molecules in batch or CO fed-batch cultivation systems that can easily reach product quantities of several

hundred moles.

3.2. Simulation of the kinetic models

In order to simulate this system, Monod equation was first modified using the K_d and K_P. Based on this model, the overall microbial kinetics were simulated using a variety of $k_L a$. Although μ appeared to be a major parameter, it was significantly affected by C_{co}, determined by the gas–liquid mass transfer and microbial activity of the cultivation system.

Time course measurements for μ were simulated using the maximum specific growth rate (μ_{max}) determined from the experimental data. K_d of 0.002 /hr was selected by comparing the experimental and simulated values. A k_La of 13 /hr was used based on the results presented in Fig. 3 (A). The kinetic parameters, constants, and yield coefficients are summarized in Table 2.

As shown in Fig. 2 graphs using (C_{co}≠0) condition , the overall simulated lines agreed with the experimental data from 13 to 20 /hr k_La; however, the simulation slightly underestimated the log phase growth at a k_La of 13 /hr because the yield coefficient measurements were obtained using only log phase data and not end point. predicted and measured overall *X* in Fig. 2 (A) were slightly inconsistent. As a result, a normalized root mean square value (NRMSE) of 6.76 % was obtained. In case of a k_La of 20 /hr, overall trend during log phase showed better fitting than that of a k_La of 13 /hr, but overestimation occurred over 24 hr. Headspace CO_2 showed a good agreement with experimental data at 20 /hr, resulting in 4.1 % NRMSE that is the second lowest value in NRMSE analysis of all the results simulated in this study. The NRMSE values of the simulations using ($C_{co} \neq 0$) condition was summarized in Table 3. In the case of acetate in Fig. 2 (C), the final *Cace* of 19.83 mM was 10.7 % higher than the simulated value of 17.7 mM at a k_La of 13 /hr, leading to a 5.60 % NRMSE. *Cace* was overestimated during late log to stationary phase over a k_La of 20 /hr and reached to around 18.2 mM.

Fig. 2 (D), (E) and (F) are the simulated results using ($C_{co} = 0$) in Eqn. 6. The simulation trend was almost similar with that of ($C_{co} \neq 0$) condition up to a k_La of 3 /hr, however, the simulated line has begun to be overestimated and show a sharp change from a k_La of 6 /hr. At a k_La of 11.5 /hr, all the simulations reached to the maximum value in about 18 hr, leading to significant inconsistency compared to experimental data. It would be due to the maximized mass transfer ($k_L a \cdot P_{co} \cdot H_{co}$) without C_{co} assumption. These results actually showed higher values of NRMSE than ($C_{co} \neq 0$) condition at a similar k_La as shown in Table 4.

Fig. 2 indicated a need for appropriate assumption and accurate measurements of coefficients used to mathematical models to achieve a more precise simulation result. In order to simulate a gas cultivation system, delicate C_{co} will have to be introduced based on the mass transfer for the prediction of more accurate simulation parameters as well as μ.

3.3. Prediction of k_La of the system via the headspace CO simulation

Elaborated model is applicable under kinetically limited and non-limited condition. The differences among the various simulation results of headspace CO are highlighted in Fig. 3. Simulations were performed under two conditions ($C_{co} = 0$ and $C_{co} \neq 0$). Eqn. 7 was used to simulate the time courses of the headspace CO. In case of Fig. 3 (B), same assumption as used in Fig. 2 (D), (E) and (F) was adopted, which overestimated the gas–liquid mass transfer rate ($k_L a \cdot P_{co} \cdot H_{co}$). This effect resulted in a mismatch between the simulation trend shown in Fig. 3 (B) and the actual data, and smaller values than those plotted in Fig. 3 (A) were obtained at similar k_La. The simulated headspace CO deviation from experimental data increased, even with a slight increase in k_La. The headspace CO simulated in Fig. 3 (B) was depleted within 20 hr at a k_La of only 11.5 /hr. Also, the dramatic change in the simulation line reduced the reliability of this model. It was re-confirmed that no C_{co} assumption produced a large error in the system performance estimates as well as in the simulation, resulting in an incorrect prediction of k_La.

On the other hand, Fig. 3 (A) displayed a much more reasonable change in the headspace CO in all time courses owing to the proper operation of the model described by Eqn. 6. The C_{co} of the system simulated in Fig. 3 (A) changed over time, and the driving force ($P_{co} \cdot H_{co} - C_{co}$) for mass transfer was not maximized. The predicted k_La was a significant determinant of the overall volumetric gas–liquid mass transfer, as in the actual system. The simulation presented in Fig. 3 (A) was carried out by predicting the value of k_La that causes reduction of the headspace CO during the time course measurements. These results revealed that a system with distinct values of k_La would be characterized by quite different headspace CO decreases. The experimental time course measurements were in excellent agreement with the simulated values at a k_La of 13 /hr (NRMSE = 2.37 %), suggesting that the k_La was appropriate for conventional batch cultures used in lab-scale microbial cultivation. This method was expected to be useful for predicting the k_La of small systems without directly measuring C_{co}; however, accurate measurements of the microbial kinetic parameters would be required.

The simulation results presented in Fig. 3 also support the experimental findings that batch culture fermentation in small systems face substrate-limited conditions due to poor mass transfer (Bredwell et al., 1999; Garcia-Ochoa & Gomez, 2009; Munasinghe & Khanal, 2012; Yasin et al., 2014). In the whole reactions, the CO consumption rate achievable by microorganism exceeds the mass transfer rate achievable by gas-liquid equilibrium, and the poor mass transfer makes it impossible to maintain the dissolved CO concentration at a level capable of maximizing the microbial activity. Enhancing k_La of the vial over 13 /hr increased the overall CO consumption rate, as in the case of 50 /hr, shown in Fig. 3(A).

3.4. Simulation of the CO concentration and volumetric mass transfer rate

The headspace CO simulated at 13 /hr k_La, as shown in Fig. 3 (A), was converted to the partial pressure using Eqn. 5. The corresponding saturated CO concentrations (C^*) were

predicted using Henry's law. C_{co} was simulated given continuous microbial CO consumption ($\mu \cdot X/Y_{X/CO}$), as expressed in Eqn. 6.

Fig. 4, shows that C_{co} reached near-saturation levels at 0 hr. After inoculation with the microbial source, the CO consumption induced the decline in C_{co} to a specific level such that the net q_{co} and R were nearly equal at 0 h. The net CO consumption gradually increased over time due to cell growth. As a result, the gap between C_{co} and C^* increased, thereby increasing the driving force for mass transfer. q_{co} was slightly larger than R. This trend continued to the mid-log phase, and maximized values of R and q_{co} were achieved at 16 hr, as indicated by the dotted lines. After this stage, R and CO consumption began to decrease sharply by the insufficient CO partial pressure. Keeping the mass transfer rate and cell growth rate high required a large driving force; however, during the middle stage of cultivation, the CO partial pressure remaining in the headspace dropped. Finally, C^* could not be kept as high as the early stages of the cultivation. C_{co} was maintained below 0.05 mM after 18 hr. Under these conditions, serious cell growth and CO consumption limitation occurs. The gap between q_{co} and R was gradually decreased as shown in the ellipse directed by an arrow in Fig. 4, indicating that the dependence of the cell growth on the gas–liquid mass transfer increased.

3.5. Significance of study and future research directions

Conventional methods for evaluating the k_La involves indirect measurement of C_{co} through gas chromatography, and enzyme assay (Munasinghe & Khanal, 2014). Challenges for their real applications are listed in table 6. This is the first study which proposed a way to predict the k_La and C_{co} under biotic conditions for batch systems which can be modified for continuous systems. Time course estimation of C_{co} levels during continuous fermentation may help to maintain the optimum C_{co} levels for ideal bioreactor operation.

Summary of equations used to model mass transfer and microbial growth during gas-liquid fermentation is listed in Table 5. All the previous studied are based on the saturated gas

concentrations with assumption of zero C_{co} levels during time course batch fermentation (Hwang et al., 2007; Mohammadi et al., 2014; Phillips et al., 1993; Younesi et al., 2005). However, continuous microbial substrate consumption during batch fermentations reduces the head space partial pressure of the gas in the head space (C_{gas}) which in turn lead to significant reduction of net C_{co} levels as depicted in Fig. 4. Since μ and q_{CO} depends upon the concentration of dissolved substrates (Jeong et al., 2016), evaluation of μ and q_{CO} while considering zero C_{co} levels (Younesi et al., 2005), would possibly result in an inaccurate estimation of kinetic parameters. Also, the model in Muhammadi et al., 2014 didn't reflect the microbial CO consumption ($\mu \cdot X/Y_{X/CO}$). Kinetic model proposed in this study incorporate potential influential parameters that significantly affect microbial growth and net mass transfer during batch fermentation. Furthermore, models proposed in this study can be applied to mass transfer limited to non-limited systems with actual C_{co} levels.

4. Conclusions

This study proposed a kinetic model of batch fermentation systems that utilized gaseous substrates to predict the dynamic behavior of gas molecules. These results revealed that vial-scale cultivation could be carried out at a k_La of about 13 /hr under given condition. The predicted k_La was used to simulate CO_2, acetate, and cell concentrations. The medium was not serious substrate limited condition until mid-log phase. The model proposed in this study may be used to simulate a variety of gas cultivation systems with kinetically limited and non-limited mass transfer condition.

Acknowledgements

This research was supported by grant of Center for C1 Gas Refinery for National Research Foundation (NRF-2015M3D3A1A01064883).

References

1. Ahmed, T., Semmens, M.J. 1992. The use of independently sealed microporous hollow

fiber membranes for oxygenation of water: model development. J. Membr. Sci. 69(1-2), 11-20.

2. Allman, A. 2011. Fermentation microbiology and biotechnology. CRC press.
3. Bredwell, M., Srivastava, P., Worden, R. 1999. Reactor design issues for synthesis-gas fermentations. Biotechnol. Prog. 15(5), 834-844.
4. Chang, I.-S., Kim, B.-H., Kim, D.-H., Lovitt, R.W., Sung, H.-C. 1999. Formulation of defined media for carbon monoxide fermentation by *Eubacterium limosum* KIST612 and the growth characteristics of the bacterium. J. Biosci. Bioeng. 88(6), 682-685.
5. Chang, I.S., Kim, B.H., Lovitt, R.W., Bang, J.S. 2001. Effect of CO partial pressure on cell-recycled continuous CO fermentation by *Eubacterium limosum* KIST612. Process Biochem. 37(4), 411-421.
6. Chang, I.S., Kim, D.H., Kim, B.H., Shin, P.K., Sung, H., Lovitt, R.W. 1998. CO fermentation of *Eubacterium limosum* KIST612. J. microbiol. Biotechnol. 8(2), 134-140.
7. Chang, I.S., Kim, D.H., Kim, B.H., Shin, P.K., Yoon, J.H., Lee, J.S., Park, Y.H. 1997. Isolation and identification of carbon monoxide utilizing anaerobe. *Eubacterium limosum KIST612*. Korean J. Appl. Microbiol. Biotechnol. 25(1), 1-8.
8. Doran, P.M. 1995. Bioprocess engineering principles. Academic press.
9. Garcia-Ochoa, F., Gomez, E. 2009. Bioreactor scale-up and oxygen transfer rate in microbial processes: an overview. Biotechnol. Adv. 27(2), 153-76.
10. Han, K., Levenspiel, O. 1988. Extended Monod Kinetics for Substrate, Product, and Cell inhibition. Biotechnol. Bioeng. 32, 430-437.
11. Hwang, J.W., Choi, Y.B., Park, S., Choi, C.Y., Lee, E.Y. 2007. Development and mathematical modeling of a two-stage reactor system for trichloroethylene degradation using *Methylosinus trichosporium* OB3b. Biodegradation, 18(1), 91-101.
12. Jeong, Y., Jang, N., Yasin, M., Park, S., Chang, I.S. 2016. Intrinsic kinetic parameters of

Thermococcus onnurineus NA1 strains and prediction of optimum carbon monoxide level for ideal bioreactor operation. Bioresour. Technol. 201, 74-9.

13. Jones, S.T. 2007. Gas-liquid mass transfer in an external airlift loop reactor for syngas fermentation. Iowa State University.
14. Kovárová-Kovar, K., Egli, T. 1998. Growth kinetics of suspended microbial cells: from single-substrate-controlled growth to mixed-substrate kinetics. Microbiol. Mol. Biol. Rev. 62(3), 646-666.
15. Kundu, S., Premer, S.A., Hoy, J.A., Trent, J.T., Hargrove, M.S. 2003. Direct measurement of equilibrium constants for high-affinity hemoglobins. Biophys. J. 84(6), 3931-3940.
16. Lin, S.K.C., Du, C., Koutinas, A., Wang, R., Webb, C. 2008. Substrate and product inhibition kinetics in succinic acid production by *Actinobacillus succinogenes*. Biochem. Eng. J. 41(2), 128-135.
17. Merchuk, J., Asenjo, J. 1995. The Monod equation and mass transfer. Biotechnol. Bioeng. 45(1), 91-94.
18. Merkel, W., Krauth, K. 1999. Mass transfer of carbon dioxide in anaerobic reactors under dynamic substrate loading conditions. Water Res. 33(9), 2011-2020.
19. Mohammadi, M., Mohamed, A.R., Najafpour, G.D., Younesi, H., Uzir, M.H. 2014. Kinetic studies on fermentative production of biofuel from synthesis gas using *Clostridium ljungdahlii*. The Sci. World J. 2014.
20. Munasinghe, P.C., Khanal, S.K. 2010. Biomass-derived syngas fermentation into biofuels: Opportunities and challenges. Bioresour. Technol.101(13), 5013-22.
21. Munasinghe, P.C., Khanal, S.K. 2014. Evaluation of hydrogen and carbon monoxide mass transfer and a correlation between the myoglobin-protein bioassay and gas chromatography method for carbon monoxide determination. RSC Adv. 4, 37575-81.

22. Munasinghe, P.C., Khanal, S.K. 2012. Syngas fermentation to biofuel: evaluation of carbon monoxide mass transfer and analytical modeling using a composite hollow fiber (CHF) membrane bioreactor. Bioresour. Technol. 122, 130-6.

23. Phillips, J., Klasson, K., Clausen, E., Gaddy, J. 1993. Biological production of ethanol from coal synthesis gas. Appl. Biochem. Biotechnol. 39(1), 559-571.

24. Ramachandriya, K.D., Kundiyana, D.K., Sharma, A.M., Kumar, A., Atiyeh, H.K., Huhnke, R.L., Wilkins, M.R. 2016. Critical factors affecting the integration of biomass gasification and syngas fermentation technology. AIMS Bioeng. 3(2), 188-210.

25. Riggs, S.S., Heindel, T.J. 2006. Measuring carbon monoxide gas—liquid mass transfer in a stirred tank reactor for syngas fermentation. Biotechnol. Prog. 22(3), 903-906.

26. Vega, J., Antorrena, G., Clausen, E., Gaddy, J. 1989a. Study of gaseous substrate fermentations: carbon monoxide conversion to acetate. 2. Continuous culture. Biotechnol. Bioeng. 34(6), 785-793.

27. Vega, J.L., Clausen, E.C., Gaddy, J.L. 1989b. Study of gaseous substrate fermentations: Carbon monoxide conversion to acetate. 1. Batch culture. Biotechnol. Bioeng. 34(6), 774-784.

28. Verma, D., Singla, A., Lal, B., Sarma, P.M. 2016. Conversion of biomass-generated syngas into next-generation liquid transport fuels through microbial intervention: potential and current status. Curr. Sci. 110(3), 329-336.

29. Wang, G., Wang, D.I. 1984. Elucidation of growth inhibition and acetic acid production by *Clostridium thermoaceticum*. Appl. Environ. Microbiol. 47(2), 294-298.

30. Yasin, M. 2015. High Gas-Liquid Mass Transfer Bioreactor for Mirobial Syngas Utilization, Ph. D Thesis, Gwangju Institute of Science and Technology.

31. Yasin, M., Jeong, Y., Park, S., Jeong, J., Lee, E.Y., Lovitt, R.W., Kim, B.H., Lee, J., Chang, I.S. 2015. Microbial synthesis gas utilization and ways to resolve kinetic and

mass-transfer limitations. Bioresour. Technol. 177, 361-74.

32. Yasin, M., Park, S., Jeong, Y., Lee, E.Y., Lee, J., Chang, I.S. 2014. Effect of internal pressure and gas/liquid interface area on the CO mass transfer coefficient using hollow fibre membranes as a high mass transfer gas diffusing system for microbial syngas fermentation. Bioresour. Technol. 169, 637-43.
33. Younesi, H., Najafpour, G., Mohamed, A.R. 2005. Ethanol and acetate production from synthesis gas via fermentation processes using anaerobic bacterium, *Clostridium ljungdahlii*. Biochem. Eng. J. 27(2), 110-119.
34. Zhang, J., Taylor, S., Wang, Y. 2016. Effects of end products on fermentation profiles in *Clostridium carboxidivorans* P7 for syngas fermentation. Bioresour. Technol. 218, 1055-63.
35. Zhao, Y., Haddad, M., Cimpoia, R., Liu, Z., Guiot, S.R. 2013. Performance of a *Carboxydothermus hydrogenoformans*-immobilizing membrane reactor for syngas upgrading into hydrogen. Int. J. Hydrog. Energy 38(5), 2167-2175.

Table 1. Initial conditions used to simulate the batch system pressurized under 1 atm CO/CO_2 (8:2)

Initial condition	Unit	Value
X_0	mg/L	24.39
$C_{ace,0}$	mmol/L	0.875
$C_{co,0}$	mmol/L	0.654
$N_{co_2,0}$	mmol	0.920
$N_{CO,0}$	mmol	4.002

Table 2. Kinetic parameters, constants, yield coefficients describing *E. limosum* KIST612 growth, and the simulated $k_L a$ value

Kinetic parameter	Unit	Value	Reference
μ_{max}	/hr	0.165	Determined by batch test data from (Chang et al., 1999)
K_d	/hr	0.002	Fitted to batch test data from (Chang et al., 1999)
$k_L a$	/hr	13	Fitted to experimental data
Constant			
K_S	mmol/L	0.082	(Chang et al., 2001)
K_p	mmol/L	744.3	Determined by extrapolation of experimental data
Yield coefficient			
$Y_{ace/CO}$	-	0.173	Determined by batch test data from (Chang et al., 1999)
$Y_{CO_2/CO}$	-	0.504	Determined by batch test data from (Chang et al., 1999)
$Y_{X/CO}$	mg/mmol	4.752	Determined by batch test data from (Chang et al., 1999)

Table 3. Normalized root mean square error (NRMSE) of simulated parameters using various $k_L a$ values with ($C_{co} \neq 0$) condition

$k_L a$ (/hr)	NRMSE (%)			
	X	N_{co}	N_{co_2}	C_{cae}
1	53.9	47.75	50.42	47.38
3	33.46	28.59	31.83	29.92
6	18.47	14.06	17.76	16.69
9	11.12	6.54	10.44	9.9
13	6.76	2.37	5.44	5.6
20	6.23	5.69	4.1	5.07
30	8.3	9.12	6.44	7.21
50	10.77	12.04	9.07	9.57

Table 4. Normalized root mean square error (NRMSE) of simulated parameters using various $k_L a$ values with ($C_{co} = 0$) assumption

$k_L a$ (/hr)	NRMSE (%)			
	X	N_{co}	N_{co_2}	C_{cae}
1	52.76	46.73	49.42	46.45
3	27.75	23.67	26.93	25.45
6	5.87	6.21	8.39	8.75
9	10.54	13.5	10.35	10.98
11.5	18.87	20.94	17.16	17.17

Table 5. Comparison of microbial growth and mass transfer model related with gases substrate

Growth and mass transfer kinetic model	Reference
$\frac{dC_{\text{gas}}}{dt} = k_L a \cdot C^*$	(Hwang et al., 2007)
$-\frac{1}{V_L}\frac{dN_{CO}}{dt} = \frac{k_L a}{H} P_{CO}$	(Mohammadi et al., 2014; Phillips et al., 1993)
$P_{CO} = P_{CO,0} \cdot e^{k_P t}$ $\mu = \frac{\mu_{max} \cdot P_{CO}}{K_S + P_{CO} + (P_{CO})^2/K_i}$	(Mohammadi et al., 2014)
$\mu = \frac{\mu_{max} \cdot C^*}{K_S + C^* + (C^*)^2/K_i}$	(Younesi et al., 2005)
$\mu = \frac{\mu_{max} \cdot C_{co}}{(K_S + C_{co}) \cdot (1 + C_{ace}/K_P)} - K_d \cdot \left(1 + \frac{C_{ace}}{K_P}\right)$ $\frac{dC_{co}}{dt} = k_L a \cdot (P_{co} \cdot H_{co} - C_{co}) - \mu \cdot X/Y_{X/CO}$	This study

k_P Constant for 1st-order decrease in headspace CO

Table 6. C_{CO} **measurement methods and challenges associated with them**

Method	Challenges	Reference
Direct GC measurement	➢ Online measurement is not possible ➢ Large sample loss ➢ Long measurement time ➢ Inaccuracy of measurement by gas bubbles in samples ➢ Not suitable for biotic conditions	(Chang et al., 2001; Munasinghe & Khanal, 2014; Zhao et al., 2013)
Myoglobin assay	➢ Cannot be applied for thermophilic culture due to enzyme deactivation ➢ prone to errors ➢ Require strict anaerobic conditions ➢ Not suitable for biotic conditions	(Jones, 2007; Kundu et al., 2003; Munasinghe & Khanal, 2014; Riggs & Heindel, 2006)

Figure captions

Fig. 1. Specific growth rate profile of *E. limosum* KIST612 under different acetate concentration ranges. The data obtained below 120 mM were extrapolated out to 480 mM to calculate the acetate inhibition constant (K_P). Data point that showed highest specific growth rate was used in two or three sample sets.

Fig. 2. Comparison of the simulated model of the cell concentration, headspace CO_2, and acetate, with the actual experiment data using different k_La values. Simulations were conducted under the assumption that ($C_{co} \neq 0$) and ($C_{co} = 0$) respectively. Batch cultivation data reported previously (Chang et al., 1999) were used for the simulation.

Fig. 3. Change in the headspace CO, simulated using different k_La values, and a comparison with the experimental data points. (B) was simulated under the assumption that ($C_{co} = 0$) in Eqn. 6. The headspace CO was analyzed in triplicate. Eqn. 7 was used to simulate the headspace CO. The batch cultivation data previously reported in (Chang et al., 1999) were used for the simulation.

Fig. 4. Change in the dissolved, saturated CO concentration, gas–liquid mass transfer, and microbial CO consumption rate in the medium. Saturated CO was predicted using Henry's law and the ideal gas equation based on the simulated headspace CO.

Fig. 1

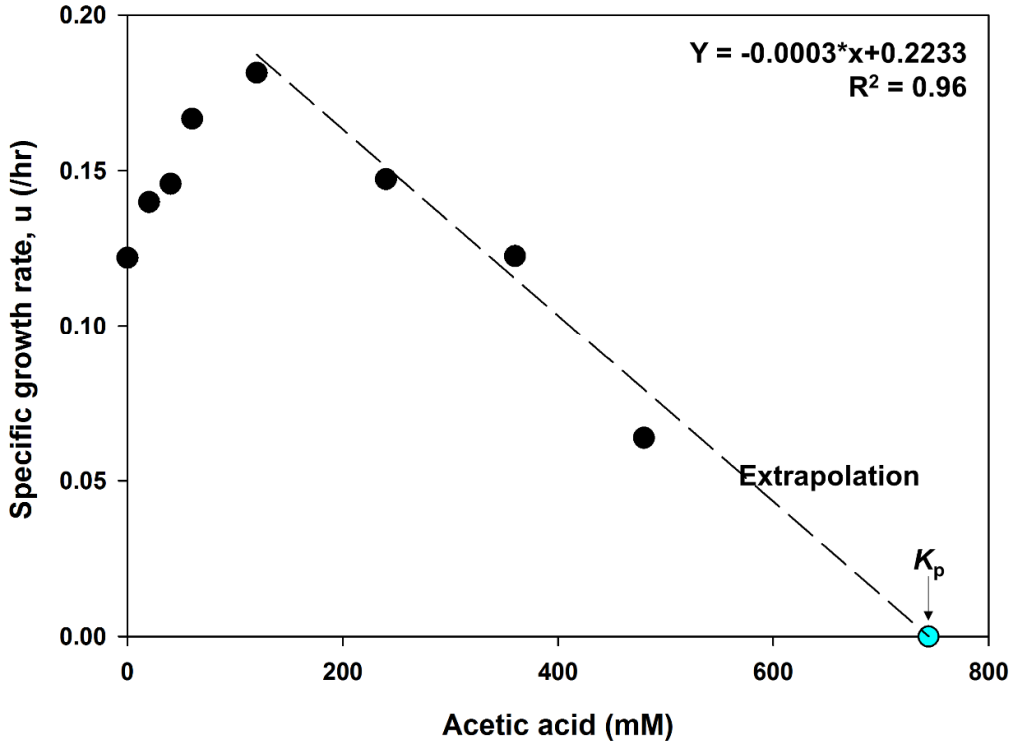

Fig. 2

Fig. 3

Fig. 4

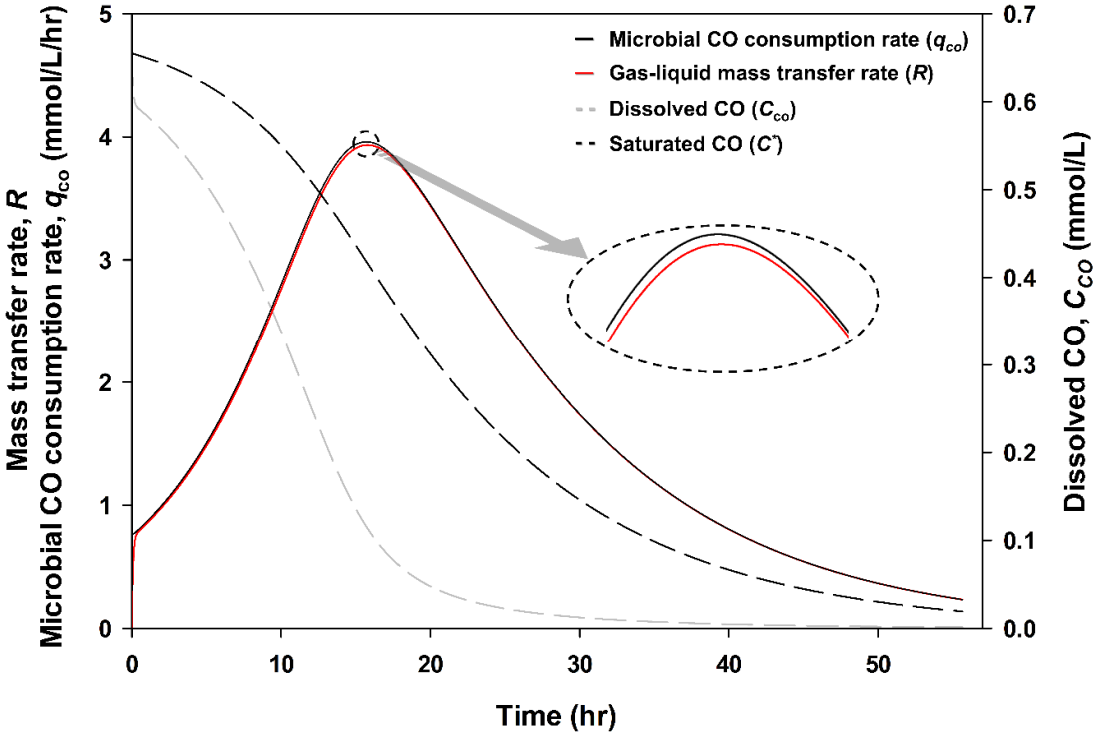

Highlights

- First report of k_La for a batch cultivation system using kinetic simulation
- Combined microbial kinetics and gas–liquid mass transfer
- The dissolved CO concentration and mass transfer in a batch system were simulated
- No dissolved CO assumption leads to a large error in simulating gas cultivation